Materials and Structures (2021) 54:209
https://doi.org/10.1617/s11527-021-01801-y

ORIGINAL ARTICLE

Flow behavior of cementitious-like suspension with nano-Fe_3O_4 particles under external magnetic field

Dengwu Jiao · Karel Lesage · Mert Yücel Yardimci · Caijun Shi · Geert De Schutter

Received: 24 May 2021 / Accepted: 29 September 2021 / Published online: 1 November 2021

Abstract The flow behavior of cementitious-like (limestone powder) suspension containing nano-Fe_3O_4 particles at constant shear rate of 10 s^{-1}, characterized by the evolution of apparent viscosity over time, is investigated under various magnetic fields. Results show that the limestone powder suspension at flow-state exhibits remarkable magneto-rheological responses, reflected by a significant increase in the apparent viscosity after applying an external magnetic field. A higher field strength corresponds to a more rapid and pronounced response. The apparent viscosity experiences a sudden alteration with the stepwise change of the magnetic field due to the formation or disintegration of magnetic clusters. Linearly increasing magnetic field strength at low ranges (e.g. 0 T–0.3 T) shows less influences on the evolution of apparent viscosity, while at relatively high magnetic field, the apparent viscosity gradually increases with the magnetic field strength and the increase rate is comparable to that obtained under constant high magnetic field of 0.75 T. When the magnetic field is removed, the apparent viscosity exhibits a sharp reduction. If the magnetic field strength linearly decreases to zero, however, the apparent viscosity continuously increases until reaching a peak and then gradually decreases. This research shows in different ways how a desired apparent viscosity level of a cementitious-like suspension can be reached by means of an external magnetic field.

Keywords Active rheology control (ARC) · Apparent viscosity · Constant shearing test · Magnetic field · Nano-Fe_3O_4 particles

D. Jiao · K. Lesage · M. Y. Yardimci · G. De Schutter (✉)
Magnel-Vandepitte Laboratory, Department of Structural Engineering and Building Materials, Ghent University, 9052 Ghent, Belgium
e-mail: Geert.DeSchutter@UGent.be

D. Jiao · C. Shi (✉)
Key Laboratory for Green and Advanced Civil Engineering Materials and Application Technology of Hunan Province, College of Civil Engineering, Hunan University, Changsha 410082, China
e-mail: cshi@hnu.edu.cn

1 Introduction

Contradicting requirements of properties always exist in different casting processes. For example, fresh concrete should possess relatively low yield stress, suitable plastic viscosity and excellent stability during pumping process [1–3]. After the concrete casting into the formwork, however, a higher yield stress is beneficial to reducing the formwork pressure and speeding up the casting process [4–6]. The contradicting property requirements also exist in 3D concrete printing concerning pumpability, extrudability and buildability [7–9]. This kind of opposing requirements

of properties poses a great challenge to the construction technique of concrete.

Active rheology control is a ground-breaking concept targeting at controlling the structural evolution and rheological properties to meet the property requirements in different processes for the same concrete mixture [10, 11]. Differing from traditional control methods by adding mineral additives or chemical admixtures [12–14], active rheology control is achieved by artificially activating an external trigger signal to cementitious materials with responsive admixtures [15]. This means that active rheology control is a post-mixing control method. A typical trigger signal used in cementitious materials is magnetic field, where magnetizable particles or functional admixtures can be used as the responsive additives, named as magneto-rheology control [16–18]. In addition to magnetic field, other signals can also be used to control the rheological properties of cement-based materials, as illustrated for an example in [19]. Active rheology control has a potential to become the mainstream of future casting techniques of cementitious materials [20].

With regard to magneto-rheology control, it is evident that the structural build-up of fresh cementitious paste with magnetic particles can be adjusted by using an external magnetic field [21–23]. Applying a magnetic field promotes the movement of magnetic particles and creates a micro-agitation effect, leading to an increase in the early liquid-like behavior of cement paste [24, 25]. After a longer period of magnetization, the cement paste shows an improvement in stiffness because of the formation of magnetic clusters [26]. The structural build-up of cementitious paste under a magnetic field is mainly determined by the magnetic properties and crystalline structures of the nano-Fe_3O_4 particles, rather than their particle size [27]. Besides, the magnetic field itself has a significant influence on the structural build-up of cementitious paste. An abrupt decrease in storage modulus can be observed when increase the magnetic field strength from low to high value, and after removal of the magnetic field, the cementitious paste shows a relatively faster structural build-up [22].

For the dynamic flow properties, previous experimental results show that the measured shear stress of nano-Fe_3O_4 incorporated cementitious paste under a magnetic field of 0.5 T is even lower than that obtained without magnetic field due to the obvious nanoparticle agglomeration and bleeding in the interface between the cementitious paste and the upper rotating plate [28]. This results in an inaccurate evaluation of yield stress and plastic viscosity. By examining the magnetic properties of the hardened cementitious paste powders in the plate, it is revealed that the nanoparticle agglomeration is contributed by the combined effect of high magnetic field and high-rate shearing. Considering the future applications of magneto-rheology control in concrete pumping, advanced rheological protocol should be used to understand the effect of magnetic field on the rheological properties of cementitious materials at flow-state.

In the present study, the flow behavior of cementitious-like suspension containing nano-Fe_3O_4 particles at constant shear rate of 10 s^{-1} is investigated under various magnetic fields. The constant low-rate shearing limits the migration and agglomeration of nanoparticles in the suspension. Limestone powder suspension is selected, as it exhibits similar rheological behavior to cementitious suspension. The further advantage of this suspension is that only physical interactions such as van der Waals forces and magnetic forces exist, excluding the chemical effect on the early shearing test. Several modes of magnetic fields, including constant magnetic fields, step-changed magnetic fields, and linear-changed magnetic fields, are separately applied to the suspension under constant low-rate shearing. The evolution of apparent viscosity over time, representing the response of the suspension to an external magnetic field, is illustrated and theoretically discussed from the viewpoint of particle interactions.

2 Experimental program

2.1 Materials and sample preparation

De-ionized water and limestone powder (LP) with average particle size (D_{50}) of 3.71 μm and specific gravity of 2.70 were utilized. The particle size distribution of the limestone powder is shown in Fig. 1. Commercial spherical iron oxide nanoparticles (MNPs) with Fe_3O_4 purity higher than 98%, purchased from US Research Nanomaterials, Inc, were used. According to the manufacturer, the nano-Fe_3O_4 particles have an average particle size of 20–30 nm and a

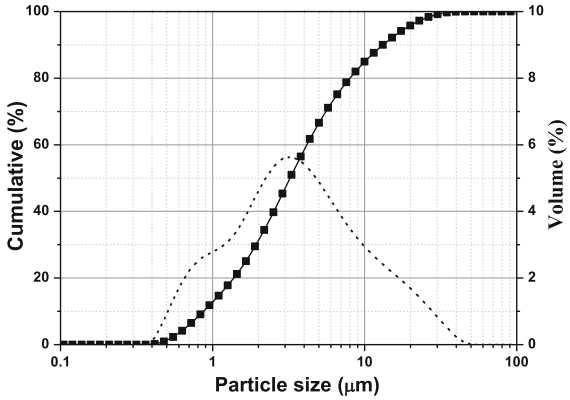

Fig. 1 Particle size distribution of the limestone powder

specific gravity of 4.95. The magnetization curve of the nanoparticles obtained from a vibrating sample magnetometer is presented in Fig. 2.

A typical limestone powder suspension with W/LP of 0.35 and MNPs content of 3% (by mass of limestone powder + water) was selected. The low water content ensures excellent stability and appropriate flowability of the suspension. The suspension was mixed using a rotational rheometer (MCR 52, Anton Paar) equipped with a helix geometry. The geometric parameters of the helix rotator and the mixing procedure are the same as given in [17, 22]. Note that the high rotational speed of 3000 rpm provides a repeatable initial state of paste samples.

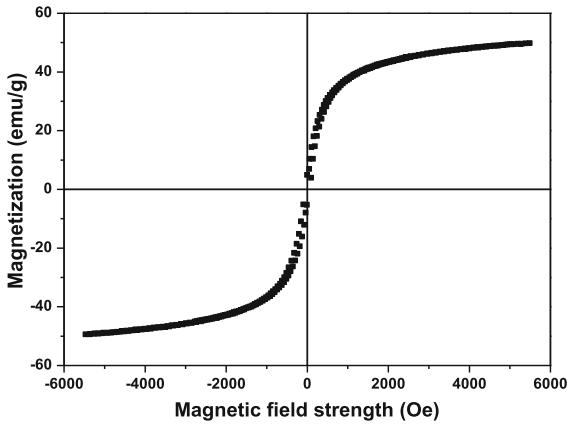

Fig. 2 Magnetization versus magnetic field strength curve of the nano-Fe_3O_4 particles

2.2 Testing methods

The flow behavior of the suspension was assessed using a rotational parallel plate rheometer (MCR 102, Anton Paar). A magneto-rheological device (Physica MRD 170 + H-PTD200) is equipped to generate a uniform magnetic field perpendicular to the plates [29, 30]. The magnetic flux density can be controlled by inputting the current in the coil. The effective diameter of the plate is 20 mm. During the rheological test, the gap between the upper and lower plates was fixed at 1 mm, and the temperature was maintained at 20 ± 0.5 °C.

After pouring the sample onto the plate of the rheometer, a pre-shearing procedure with a shear rate of 100 s^{-1} was first applied for 30 s, followed by 10 s resting time. The purpose of the pre-shearing is to destroy the possible agglomeration structures and obtain a reference state. Note that no magnetic field was applied during the pre-shearing and resting. Subsequently, a constant shearing test with a shear rate of 10 s^{-1} was performed under a specific magnetic field and the shear stress was recorded every two seconds. The selected magnetic field strength will be illustrated in the following sections. The surface of the suspension in the plate was checked after the rheological test, and there was no obvious bleeding or nanoparticle agglomeration observed. The apparent viscosity results from the measured shear stress as follows:

$$\mu = \frac{\tau}{\dot{\gamma}} \tag{1}$$

where μ is the apparent viscosity (Pa.s), τ is the measured shear stress (Pa), and γ is the shear rate (=10 s^{-1}). Three test repetitions were conducted for each batch using remixed paste. The error bar in the following figures indicates the standard deviation calculated from the three obtained results.

3 Results and discussion

3.1 Constant magnetic fields

3.1.1 Evolution of apparent viscosity

Figure 3 presents the influence of constant magnetic fields on the evolution of apparent viscosity of the

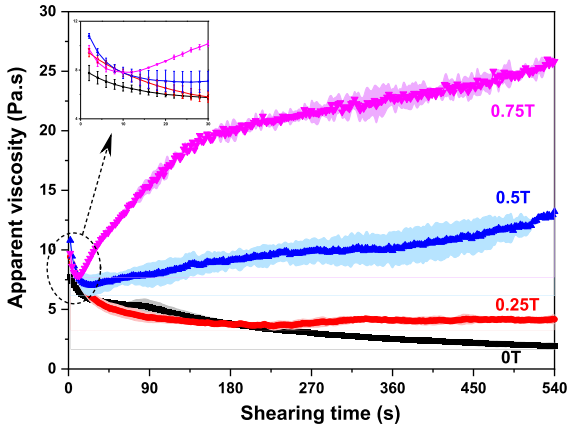

Fig. 3 Evolution of apparent viscosity of the suspension under constant magnetic fields, at constant shear rate of 10 s^{-1}

limestone powder suspension at constant shear rate of 10 s^{-1}. Four constant magnetic fields with strength of 0 T, 0.25 T, 0.5 T and 0.75 T were exerted on the suspension at the beginning of the shearing. In the absence of magnetic field, the suspension exhibits a significant reduction in the apparent viscosity immediately after initiation of the shearing. There is an obvious decay in the apparent viscosity followed by an approximate steady-state after a longer period of shearing. The initial reduction of the apparent viscosity can be explained by the breakdown of flocculated structures between solid particles formed in the resting period. The decay of the apparent viscosity results from the competition between the formation of internal flocculates due to colloidal interactions and the structural breakdown because of thermal motion and hydrodynamic forces.

In the presence of an external magnetic field, the development of apparent viscosity with time shows distinct behavior, due to the rheological response of the suspension to the magnetic field. On the one side, it can be seen from the inserted enlarged view in Fig. 3 that the initial apparent viscosity of the suspension under an external magnetic field, irrespective of the magnetic field strength, is slightly higher than that obtained without magnetic field. This implies that the magnetic clusters of nanoparticles are formed immediately after applying an external magnetic field. On the other side, under constant shearing, the hydrodynamic forces tending to destroy the internal structures compete with the interactions facilitating the buildup of colloidal structures and magnetic clusters. Therefore, the apparent viscosity at constant shear rate tends to evolve differently, depending on the strength of the magnetic field. Indeed, under a weak magnetic field of 0.25 T, the apparent viscosity gradually decreases at early shearing time. This means that the formation of colloidal structures and magnetic clusters is not predominant. After shearing for around 230 s, the apparent viscosity shows slightly higher magnitude than that under zero magnetic field. This can be attributed to the fact that the shearing operation possibly facilitates the formation of magnetic clusters of nano-Fe_3O_4 particles in the suspension [28], exerting a slight resistance to the shear flow. By comparison, under a magnetic field with relatively high strength such as 0.75 T, the suspension exhibits a more pronounced response to the magnetic field. Specifically, the apparent viscosity shows a decrease at the beginning of the shearing due to the breakdown of flocculates. After a few seconds of shearing, the studied suspension exhibits a rapid increase in the apparent viscosity. This indicates that the colloidal flocculation and magnetic clusters formation are predominant. After experiencing longer shearing under magnetic field, the apparent viscosity shows a steady increasing trend, indicating an equilibrium between structural build-up and breakdown. It should be noticed that the structural build-up mainly contributed by the formation of magnetic clusters is still dominant in this stage.

Furthermore, it can be observed from Fig. 3 that a higher magnetic field strength corresponds to a more rapid response of the suspension under constant shearing at 10 s^{-1}. Indeed, the suspension starts to respond at shearing time around 230 s under a magnetic field of 0.25 T. However, in the presence of a magnetic field of 0.75 T, the apparent viscosity of the suspension exhibits a significant increase at around 10 s. Besides, the apparent viscosity at the shearing time of 540 s raises from 1.9 to 25.8 Pa.s with increasing magnetic field strength from 0 to 0.75 T. The non-linear increase of the apparent viscosity with magnetic field strength can possibly be attributed to the viscoelastic properties of the suspension [31]. Nevertheless, applying a constant magnetic field increases the viscosity of the limestone powder suspension containing nano-Fe_3O_4 particles under constant shearing state.

3.1.2 Theoretical discussions

The fresh limestone powder paste with nanoparticles can be regarded as a concentrated suspension with solid particles suspending in a continuous fluid phase (i.e. water). The particle size of the solid grains varies from several nanometers to tens of micrometers. In the absence of external magnetic field, several types of particle interactions are present in the poly-disperse suspensions at flow-state, which can be summarized as non-contact forces or colloidal interactions, Brownian forces, hydrodynamic forces, and contact forces between solid particles [32].

The non-contact (colloidal) interactions in a concentrated suspension include van der Waals forces, electrostatic double layer forces, and/or steric hindrance repulsion [22, 33]. The magnitude of each force depends on the separation distance between solid particles. In the case of the studied limestone powder suspension without chemical polymers, the van der Waals attractive forces F_{VDW}, as expressed in Eq. (2), are assumed to dominate all other colloidal interactions.

$$F_{VDW} = \frac{A_0 d}{12H^2} \tag{2}$$

where A_0 is the Hamaker constant (J), d is the particle diameter (m), and H is the surface-surface separation distance (m).

Brownian motion is the random thermal agitation of solid particles in a suspension. The Brownian forces of particles with size only lower than a few micrometers have significant importance for the properties of the suspension, causing the fine particles to randomly diffuse in the suspending phase. A dimensionless parameter N_r estimating the relative magnitude of Brownian motion over inter-particle force is expressed by Eq. (3) [34]:

$$N_r = \frac{A_0 d}{12H \cdot kT} \tag{3}$$

where k is the Boltzman constant ($m^2.kg.s^{-1}.K^{-1}$), and T is the absolute temperature (K). If N_r is higher than 1, the thermal agitation is negligible compared with the van der Waals attractive forces. For conventional cementitious suspensions without polymers and ultrafine additives, Brownian motion can be neglected compared to the colloidal interactions [35].

For suspensions at flow state, a particle in the suspension experiences a hydrodynamic force tending to facilitate the particle to move. Meanwhile, a viscous drag force is applied on the particle to dissipate the kinetic energy. In the case of a spherical particle in a shear field, the magnitude of the hydrodynamic force is proportional to the square of the particle diameter (d^2) [36]. The hydrodynamic force F_H exerted by the shear field on a particle can be calculated using Eq. (4).

$$F_H = \frac{3}{2}\pi\eta_s d^2\dot{\gamma} \tag{4}$$

where η_s is the viscosity of the carrier fluid (Pa.s), d is the particle diameter (m), and γ is the shear rate (1/s).

In the presence of an external magnetic field, magnetic forces exist between magnetic nanoparticles, facilitating the nanoparticles tending to form magnetic clusters [24, 26]. Assuming that all the nanoparticles have the same constant dipole moment and are arranged in the voids between limestone particles in simple cubic order, upon the beginning of applying an external magnetic field, the magnetic force F_M of two individual nanoparticles with center line along the direction of the magnetic field can be estimated by Eq. (5) [24]:

$$F_M = \frac{\pi d^2 \mu_0 (\rho M)^2}{24} \cdot \left(\frac{6\phi_{MNPs}}{\pi}\right)^{\frac{4}{3}} \tag{5}$$

where d is the particle size of the nano-Fe_3O_4 particles (m), ρ and M are respectively the density (kg/m^3) and magnetization per unit mass (Am^2/kg) of the magnetic nanoparticles, μ_0 is the magnetic permeability of the medium (assumed to be the same value of vacuum, i.e. $4\pi \times 10^{-7}$ N/A^2), and Φ_{MNPs} is the volume fraction of nanoparticles relative to the voids between limestone particles, which can be calculated as:

$$\phi_{\mathrm{MNPs}} = \frac{V_{\mathrm{MNPs}}}{(1-\phi_{\mathrm{LP}}) \cdot V_{\mathrm{Total}}} \tag{6}$$

where Φ_{LP} is the volume fraction of limestone particles (%). V_{MNPs} and V_{Total} are the volume of magnetic nanoparticles and total limestone powder paste (kg/m^3), respectively. The estimated magnetic force is an important indicator to evaluate the interactions between two nanoparticles upon applying a

magnetic field [24]. It should be mentioned that the estimated magnetic force is not the real numerical force between magnetic nanoparticles.

Based on the aforementioned theoretical equations, the intensity of various inter-particle connections in the limestone powder suspension is evaluated. For simplicity, the interactions between nanoparticles and limestone particles are neglected, in spite of their potential influence on the performances of the suspension. In other words, only the forces between two adjoining nano-Fe_3O_4 particles or two neighboring limestone particles are taken into account. The van der Waals force is first estimated. According to [37], the Hamaker constant for the interactions between non-metallic solids and water is typically in the range of 1.0–1.5 $\times$ 10^{-20} J. The surface-surface separation distance between limestone particles is assumed to be 0.1 μm [38]. In the case of neighboring nanoparticles, the distance can be estimated based on the assumption of simple cubic packing of the nanoparticles in the voids between limestone powder particles [24, 27], around 46 nm in this study. Afterwards, the relative magnitude of Brownian motion over inter-particle force is estimated, with the Boltzman constant equal to 1.381 $\times$ 10^{-23} $m^2.kg.s^{-2}.K^{-1}$ and the absolute temperature of 293 K. At constant shear rate of 10 s^{-1}, the hydrodynamic forces between solid particles can be calculated according to Eq. (4) with the viscosity of the medium (i.e. water) of 0.001 Pa.s at 293 K. After applying an external magnetic field, the magnetic force between two adjoining nanoparticles is then estimated. As can be seen from Fig. 2, the magnetization of the nanoparticles tends to saturate even at low magnetic field strength, where the suspension shows insignificant magneto-rheological responses due to its intrinsic viscoelastic properties [25], so that the saturation magnetization is selected as the value of M in Eq. (5). It should be mentioned here that the inter-particle connections because of the external magnetic field gradually increase with magnetization time (and/or magnetic field strength) due to the contact of the nanoparticles as well as the size increase of clusters of nanoparticles. The main parameters and the order of magnitude of the calculated interactions are summarized in Table 1.

In the absence of external magnetic field, Brownian motion and hydrodynamic forces tend to destroy the internal microstructures constructed by the colloidal interactions, i.e. van der Waals attractive forces. As expected, the Brownian forces between limestone particles can be neglected compared with the van der Waals forces, while the hydrodynamic forces between individual nanoparticles are negligible. Under constant shearing at 10 s^{-1}, it can be seen from Table 1 that the colloidal interactions cannot play a dominant role in the suspension. This indicates that the internal microstructure can be gradually destroyed by the constant shearing, which is consistent with the gradual decrease in the apparent viscosity in Fig. 3. Under an external magnetic field, the magnetic forces between nanoparticles always dominate the Brownian motion [39]. Furthermore, it can be seen from Table 1 that the colloidal interactions and the magnetic forces dominate the hydrodynamic forces. This dominance will be amplified with the increase of the interactions between clusters. Besides, higher magnetic field strength results in more nanoparticles contributing to the magnetic clusters, and thus higher magnetic force between nanoparticles [26, 27]. Accordingly, the structural formation plays a more significant role than the structural breakdown, reflected by the considerable increase in the apparent viscosity under high magnetic fields. The above-stated theoretical estimations provide preliminary explanations for the change of apparent viscosity of the suspension under the synergistic effect of constant shearing and magnetic field.

3.2 Time-varying magnetic fields

3.2.1 Step-changed magnetic fields

This section discusses the apparent viscosity evolution of the limestone powder suspension imposed to step-changed magnetic fields at constant shear rate of 10 s^{-1}. Step-increased (0 T–0.5 T–0.75 T) and step-decreased (0.75 T–0.5 T–0 T) magnetic fields were selected. Each stage of the applied magnetic field lasted for 180 s. The development of apparent viscosity of the suspension under the synergistic effect of step-changed magnetic field and constant shearing is presented in Fig. 4.

Under the step-increased magnetic field at constant shear rate of 10 s^{-1}, the apparent viscosity exhibits a rapid increase when the magnetic field increases from low to high value, as shown in Fig. 4a, indicating an immediate enhancement in the structuration of the suspension. This behavior is totally different from the evolution of storage modulus in [22], which shows an

Table 1 Summary of the order of magnitude of the estimated interactions

Interactions	Main parameters				
Van der Waals force	Solid	d (m)	A_0 (J)	H (m)	F_{VDW} (N)
	MNPs	2.5×10^{-8}	$1.0 \sim 1.5 \times 10^{-20}$	4.6×10^{-8}	$\mathbf{10^{-14}}$
	LP	3.71×10^{-6}	$1.0 \sim 1.5 \times 10^{-20}$	0.1×10^{-7}	$\mathbf{10^{-13}}$

Brownian force vs Van der Waals force	Solid	d (m)	T (K)	k ($m^2.kg.s^{-2}.K^{-1}$)	Nr
	MNPs	2.5×10^{-8}	293	1.381×10^{-23}	**0.179**
	LP	3.71×10^{-6}	293	1.381×10^{-23}	**12.228**

Hydrodynamic force	Solid	d (m)	γ (1/s)	F_H (N)
	MNPs	2.5×10^{-8}	10	$\mathbf{10^{-17}}$
	LP	3.71×10^{-6}	10	$\mathbf{10^{-13}}$

Magnetic force	Solid	ρ_{MNPs} (g/cm^3)	Φ_{MNPs}	H (m)	Ms (A.m^2/kg)	F_M (N)
	MNPs	4.95	0.0228	4.6×10^{-8}	49.48	$\mathbf{10^{-13}}$

abrupt decrease to an extremely low value close to that of reference cement paste with the step-increase of magnetic field. This can be explained by the difference of measuring sensitivity between the rotating shear test and the small amplitude oscillatory shear (SAOS) technique. When the external magnetic field suddenly increases, the magnetic nanoparticles have a potential to move to form clusters in a very short time. On the one hand, the moving nanoparticles create a sort of mechanical micro-agitation, breaking down the weak connections between solid particles and further releasing the entrapped water in the agglomerated clusters. This shows a positive influence on the improvement of the liquid-like behavior of the suspension. On the other hand, the immediate formation of the magnetic clusters tends to increase the solid-like properties of the suspension. The corresponding changes of the internal microstructure can be accurately monitored by the SAOS technique. In the case of the rotating shear test, however, the small increase of the liquid-like properties possibly cannot be captured. Instead, the formed magnetic clusters exert a resistance to the shear flow immediately, resulting in a rapid increase in the apparent viscosity. Besides, under a magnetic field of 0.5 T and a constant shear rate of 10 s^{-1}, the colloidal interactions and the magnetic forces dominate the hydrodynamic forces, as shown in Table 1. Although the shearing destroys the magnetic clusters, the flowing suspension is beneficial to facilitate the contact frequency of nanoparticles and thus the formation of clusters, which should also be responsible for the increase in the apparent viscosity. The results indicate that the stability of responsive cementitious paste during pumping could be possibly improved by introducing an external magnetic field.

After shearing under magnetization for a while, the apparent viscosity starts to increase steadily, indicating the competition between the structural build-up and the structural breakdown. A higher magnetic field strength corresponds to a faster increase in the apparent viscosity and a shorter time to reach the steady increase. This is in good agreement with the results obtained under constant magnetic fields in Fig. 3, which can be attributed to the stronger connections between nanoparticles under higher magnetic fields. The results in Fig. 4a also demonstrate that after applying the step-increased magnetic field for a longer period, the obtained apparent viscosity of the suspension reaches the same level as obtained at the same magnetization time under a constant magnetic field. The slightly different evolution of the apparent viscosity from the constant field mode can be attributed to the difference in the initial state of the suspension. Nevertheless, this result means to a certain extent that the imposed history of the magnetic field has less influence on the structuration increase of the

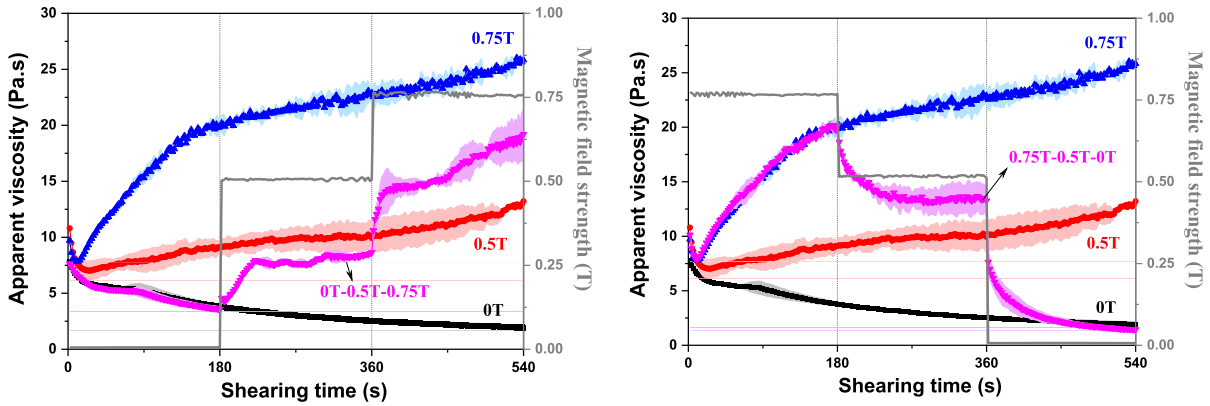

(a) Step-increased magnetic field **(b)** Step-decreased magnetic field

Fig. 4 Evolution of apparent viscosity of the suspension under step-changed magnetic fields, at constant shear rate of 10 s^{-1}

limestone powder suspension containing magnetic nanoparticles.

Figure 4b presents the influence of step-decreased magnetic field on the evolution of apparent viscosity of the limestone powder suspension under constant shearing. It can be seen that the apparent viscosity exhibits a sudden decrease with the step-decrease of the magnetic field, followed by a gradual reduction behavior. This also differs from the responses of the storage modulus, which shows a drop decrease followed by a steady increase when the magnetic field changes from high to low value [22]. The behavior of the apparent viscosity can be explained by the reversibility of the magnetic structures [21, 40]. When the magnetic field decreases, parts of the magnetic clusters disintegrate due to the reduction of magnetic forces. This leads to a decrease in the shear resistance, exhibiting a drop decline in the apparent viscosity, especially when the magnetic field decreases from 0.5 to 0 T. Under the constant shearing, it will take a relatively long period for the shearing flow to reach a new equilibrium, as reflected by the gradual decrease in the apparent viscosity. Furthermore, the apparent viscosity reduces to the same level as that obtained without magnetic field. This indicates that the residual magnetic clusters in the suspension after removing the magnetic field might be destroyed completely by the shearing.

3.2.2 Linear-changed magnetic fields

In this section, the influence of linear-changed magnetic fields on the evolution of apparent viscosity is illustrated. Three modes of linear-changed magnetic fields, as summarized in Table 2, were separately applied to the limestone powder suspension at constant shearing of 10 s^{-1}. The corresponding evolution of the apparent viscosity is presented in Fig. 5.

Figure 5a displays the evolution of apparent viscosity of the limestone powder suspension under mode I. For the first cycle of the linear-increased magnetic field, it can be observed that increasing magnetic field from 0 T to approx. 0.3 T shows less influence on the evolution of the apparent viscosity, which is in agreement with the results obtained under low constant magnetic field in Fig. 3. This can be attributed to the fact that the formed magnetic clusters at low magnetic fields play an insignificant role in the resistance to the shear flow. The apparent viscosity starts to increase at the magnetic field higher than approx. 0.3 T, and the increase rate seems to be similar to that obtained under a constant magnetic field of 0.75 T. This is probably due to the fact that changing the magnetic field tends to facilitate the formation of magnetic clusters of nanoparticles. Another possible reason is that the viscoelastic properties of the suspension slow down the movement of nanoparticles under a constant high magnetic field. The apparent viscosity of the suspension at 0.75 T by linear-increased mode is lower than that obtained under a constant magnetic field of 0.75 T. This indicates that

applying a high magnetic field to a flowing cementitious paste in a pipe might have a negative influence on the pumping pressure, while this negative effect can be reduced significantly by introducing a linear-increased magnetic field. When the magnetic field changes from 0.75 to 0 T at 180 s, the apparent viscosity exhibits a sharp reduction, which is consistent with the results in Fig. 4b. At the beginning of the second cycle of the linear-increased magnetic field, the apparent viscosity experiences an expected decrease. This can be explained by the competition between the structural build-up and the breakdown of remaining clusters and colloidal flocculates, where the structural breakdown is predominant. The experimental results also imply that the evolution of the apparent viscosity under the multiple linear-increased magnetic fields is history-independent, at least within the entire shearing duration in this study.

Figure 5b presents the development of apparent viscosity of the suspension under mode II. It can be seen that the apparent viscosity shows a sudden reduction at the beginning of applying the linearly decreased magnetic field. This is consistent with the result of applying a constant magnetic field of 0.75 T. After shearing for a few seconds, the apparent viscosity starts to increase with the continuous decrease of the magnetic field from 0.75 to 0 T, due to the formation of magnetic clusters in the suspension. Compared with the results under constant magnetic field of 0.75 T, however, a more rapid response but smaller increase rate of the apparent viscosity is observed in the case of the linear-decreased magnetic field. The more rapid response provides experimental evidence to the afore-mentioned statement that changing magnetic field (in small-scale in the case of decreasing mode) has a tendency to promote the formation of magnetic clusters of nanoparticles. By contrast, the smaller increase rate of the apparent viscosity can be explained by the gradual reduction in the interactions between magnetic clusters with the decrease of field strength. At magnetic field strength of approx. 0.63 T, the

Table 2 Application modes of the linear-changed magnetic fields

Modes	Magnetic field strength		
	0–180 s	180–360 s	360–540 s
I	0 T → 0.75 T	0 T → 0.75 T	0 T → 0.75 T
II	0.75 T → 0 T	0.75 T → 0 T	0.75 T → 0 T
III	0 T → 0.75 T	0.75 T → 0 T	0 T → 0.75 T

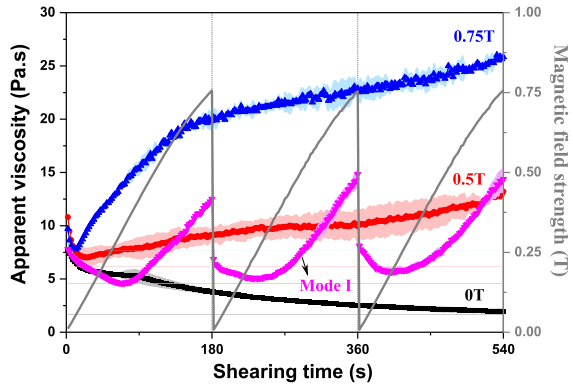

(a) Mode I

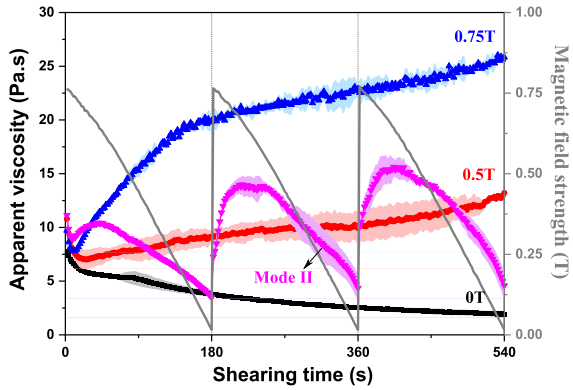

(b) Mode II

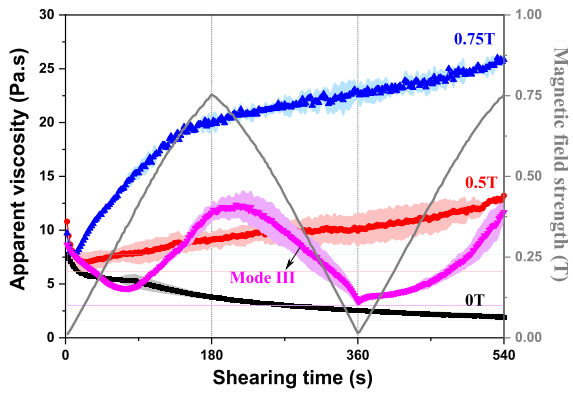

(c) Mode III

Fig. 5 Effect of linear-changed magnetic fields on the evolution of apparent viscosity, at constant shear rate of 10 s^{-1}

apparent viscosity reaches a peak and then gradually decreases. This points to the disintegration of the magnetic clusters, resulting in the structural breakdown because of the hydrodynamic forces becoming predominant. At shearing time of 180 s, the apparent viscosity experiences a sudden increase when the magnetic field changes from 0 to 0.75 T. Furthermore, the apparent viscosity shows a similar trend with linearly decreasing magnetic field for the three cycles, and the peak of the apparent viscosity always appears at magnetic field decreasing to approx. 0.63 T. This indicates that the history-independent behavior also applies to the evolution of the apparent viscosity under linear-decreased magnetic fields.

Figure 5c shows the evolution of apparent viscosity of the suspension under the magnetic field of mode III. The apparent viscosity with linearly increasing the magnetic field from 0 to 0.75 T in Fig. 5c shows the same trend as that in Fig. 5a, indicating the repeatability and reliability of the experimental results. When the magnetic field reaches 0.75 T and then starts to decrease, the apparent viscosity continuously increases within the first few tens of seconds, but the increase rate slows down. This indicates that the structural build-up due to the formation of colloidal flocculates and magnetic clusters dominates, while on the other hand, parts of magnetic clusters are decomposed simultaneously. After reaching a peak, the apparent viscosity starts to decrease with the decrease of magnetic field, probably due to the situation that the magnetic clusters gradually disintegrate and the hydrodynamic forces become to be predominant. At 360 s when the magnetic field starts to increase from 0 to 0.75 T, the apparent viscosity shows an immediate increase, which is different from the developing trend at the first cycle, or at 180 s (or 360 s) in Fig. 5a. This can be possibly attributed to the internal structure of the suspension, which is de-structured with the gradual decrease of the magnetic field, while in the case of Fig. 5a with magnetic field suddenly dropping from 0.75 to 0 T, the suspension is still in a structured state.

4 Conclusions

The flow behavior of limestone powder suspension containing nano-Fe_3O_4 particles under various magnetic fields is experimentally studied and discussed from the viewpoint of particle interactions. The current results enable to reach the following conclusions:

(1) In the absence of external magnetic field, the apparent viscosity of limestone powder suspension at constant low shear rate gradually decreases to an approximate steady state. Under constant magnetic field, the suspension exhibits obvious magneto-rheological responses due to the formation of magnetic clusters of nanoparticles. A higher magnetic field strength corresponds to a faster and more pronounced response because of the stronger connections between nanoparticles and clusters.

(2) The limestone powder suspension at flow-state shows an immediate enhancement in structuration upon applying a step-increased magnetic field, possibly due to the fact that the formation of magnetic clusters exerts an instantaneous resistance to the shear flow. The apparent viscosity of the suspension starts to increase steadily after shearing for a longer period. A step-decreased magnetic field results in a sudden decrease in the apparent viscosity, followed by a further reduction behavior.

(3) Linearly increasing magnetic field strength at low ranges (e.g. 0 T–0.3 T) shows less influence on the evolution of apparent viscosity, probably due to the weak connections between nanoparticles and/or clusters. As the magnetic field strength reaches values higher than 0.3 T, the apparent viscosity gradually increases and the increase rate is similar to that obtained under a constant high magnetic field of 0.75 T.

(4) Compared with the results under a constant magnetic field of 0.75 T, more rapid response but smaller increase rate of apparent viscosity is observed in the case of linearly decreasing magnetic field from 0.75 to 0 T due to the competition between formation and disintegration of magnetic clusters. As the magnetic field decreases to approx. 0.63 T, the apparent viscosity reaches a peak and then gradually decreases. The evolution of apparent viscosity of the suspension under linear-changed magnetic fields is history-independent.

(5) The apparent viscosity of the suspension with magnetic field changing from high value to zero shows history dependency. When the magnetic

field suddenly changes, the apparent viscosity exhibits a sharp reduction. However, if the magnetic field linearly decreases to zero, the apparent viscosity continuously increases at a decreasing growth rate within the first few tens of seconds. After reaching a peak, the apparent viscosity gradually decreases with the decrease of magnetic field strength.

Further research about applying an external magnetic field to responsive cement paste, mortar and even concrete in a real pumping system is on-going.

Acknowledgements The authors gratefully acknowledge the financial support from the European Research Council (ERC) Advanced Grant project 'SmartCast' (No. 693755).

Author Contributions Conceptualization: Dengwu Jiao and Geert De Schutter; methodology, Dengwu Jiao; software, validation, formal analysis, data curation: Dengwu Jiao and Geert De Schutter; investigation, Dengwu Jiao; resources, Karel Lesage; writing—original draft preparation, Dengwu Jiao; writing—review and editing, Karel Lesage, Mert Yücel Yardimci, and Geert De Schutter; visualization, Dengwu Jiao; supervision, Caijun Shi and Geert De Schutter; project administration, Geert De Schutter; funding acquisition, Geert De Schutter. All authors have read and agreed to the final version of the manuscript.

Funding This research was funded by ERC Advanced Grant project 'SmartCast', Grant Number 693755.

Availability of data and material All data generated or analyzed during this study are included in this published article.

Code availability Not applicable.

Declarations

Conflict of interest The authors declare that they have no conflict of interest.

Ethical approval The authors declare that they follow the rules of good scientific practice.

References

1. Kaplan D (2001) Pumping of concretes. Ph-D dissertation (in French), Laboratoire Central des Ponts et Chausées, Paris
2. Feys D, De Schutter G, Verhoeven R, Khayat KH (2010) Similarities and differences of pumping conventional and self-compacting concrete. Des Prod Placement Self-Consol Conc 2010:153–162
3. Li H, Sun D, Wang Z, Huang F, Yi Z, Yang Z, Zhang Y (2020) A review on the pumping behavior of modern concrete. J Adv Conc Technol 18(6):352–363. https://doi.org/10.3151/jact.18.352
4. Roussel N (2006) A thixotropy model for fresh fluid concretes: theory, validation and applications. Cem Conc Res 36(10):1797–1806. https://doi.org/10.1016/j.cemconres.2006.05.025
5. Roussel N (2007) Rheology of fresh concrete: from measurements to predictions of casting processes. Mater Struct 40(10):1001–1012. https://doi.org/10.1617/s11527-007-9313-2
6. Roussel N, Staquet S, Schwarzentruber LDA, Le Roy R, Toutlemonde F (2007) SCC casting prediction for the realization of prototype VHPC-precambered composite beams. Mater Struct 40(9):877–887. https://doi.org/10.1617/s11527-006-9190-0
7. De Schutter G, Lesage K, Mechtcherine V, Nerella VN, Habert G, Agusti-Juan I (2018) Vision of 3D printing with concrete: technical, economic and environmental potentials. Cem Conc Res 112:25–36. https://doi.org/10.1016/j.cemconres.2018.06.001
8. Yuan Q, Li Z, Zhou D, Huang T, Huang H, Jiao D, Shi C (2019) A feasible method for measuring the buildability of fresh 3D printing mortar. Const Build Mater 227:116600. https://doi.org/10.1016/j.conbuildmat.2019.07.326
9. Tao Y, Rahul AV, Lesage K, Yuan Y, Van Tittelboom K, De Schutter G (2021) Stiffening control of cement-based materials using accelerators in inline mixing processes: possibilities and challenges. Cem Conc Compos. https://doi.org/10.1016/j.cemconcomp.2021.103972
10. De Schutter G, Lesage K, El Cheikh K, De Schryver R, Muhammad M, Chibulu C (2017) Casting concrete structures in a smarter way. In: Proceedigns of the 14th international conference on durability of building materials and components, RILEM Proceedings PRO 107, RILEM Publications
11. De Schutter G, Lesage K (2018) Active control of properties of concrete: a (p)review. Mater Struct 51(5):123. https://doi.org/10.1617/s11527-018-1256-2
12. Reiter L, Palacios M, Wangler T, Flatt RJ (2015) Putting concrete to sleep and waking it up with chemical admixtures. Spec Publ 302:145–154
13. Marchon D, Kawashima S, Bessaies-Bey H, Mantellato S, Ng S (2018) Hydration and rheology control of concrete for

digital fabrication: potential admixtures and cement chemistry. Cem Conc Res 112:96–110. https://doi.org/10.1016/j.cemconres.2018.05.014
14. Teng L, Meng W, Khayat KH (2020) Rheology control of ultra-high-performance concrete made with different fiber contents. Cem Conc Res. https://doi.org/10.1016/j.cemconres.2020.106222
15. De Schutter G, El Cheikh K, De Schryver R, Chibulu C, Jiao D, Ezzat M, Yardimci MY, Lesage K (2019) Introduction to the concept of active rheology control in case of pumping of cementitious materials. In: Proceedings of the 2nd international RILEM conference rheology and processing of construction materials, Dresden, Germany
16. Nair SD, Ferron RD (2014) Set-on-demand concrete. Cem Conc Res 57:13–27. https://doi.org/10.1016/j.cemconres.2013.12.001
17. Jiao D (2021) Active rheology control of cementitious materials using magnetic field. Ghent University, Ghent
18. Lesage K, De Schutter G (2020) Admixture for a cementitious material to influence the rheology properties of the cementitious material. International Bureau, Universiteit Gent, Belgium
19. Sanjayan JG, Jayathilakage R, Rajeev P (2021) Vibration induced active rheology control for 3D concrete printing. Cem Conc Res 140:106293. https://doi.org/10.1016/j.cemconres.2020.106293
20. Jiao D, De Schryver R, Shi C, De Schutter G (2021) Thixotropic structural build-up of cement-based materials: a state-of-the-art review. Cem Conc Comp. https://doi.org/10.1016/j.cemconcomp.2021.104152
21. Nair SD, Ferron RD (2016) Real time control of fresh cement paste stiffening: Smart cement-based materials via a magnetorheological approach. Rheol Acta 55(7):571–579. https://doi.org/10.1007/s00397-016-0923-x
22. Jiao D, El Cheikh K, Shi C, Lesage K, De Schutter G (2019) Structural build-up of cementitious paste with nano-Fe_3O_4 under time-varying magnetic fields. Cem Conc Res 124:105857. https://doi.org/10.1016/j.cemconres.2019.105857
23. Jiao D, Lesage K, Yucel Yardimci M, Shi C, De Schutter G (2021) Possibilities of fly ash as responsive additive in magneto-rheology control of cementitious materials. Const Build Mater. https://doi.org/10.1016/j.conbuildmat.2021.123656
24. Jiao D, Lesage K, Yucel Yardimci M, El Cheikh K, Shi C, De Schutter G (2021) Rheological behavior of cement paste with nano-Fe_3O_4 under magnetic field: magneto-rheological responses and conceptual calculations. Cem Conc Comp 120: 104035. https://doi.org/10.1016/j.cemconcomp.2021.104035
25. Jiao D, El Cheikh K, Lesage K, Shi C, De Schutter G (2020) Structural build-up of cementitious paste under external magnetic fields. Rheol Proc Const Mater 2020:36–42
26. Jiao D, Lesage K, Yardimci MY, El Cheikh K, Shi C, De Schutter G (2021) Quantitative assessment of the influence of external magnetic field on clustering of nano-Fe_3O_4 particles in cementitious paste. Cem Conc Res 142:106345. https://doi.org/10.1016/j.cemconres.2020.106345
27. Jiao D, Lesage K, Yardimci MY, El Cheikh K, Shi CJ, De Schutter G (2021) Structural evolution of cement paste with nano-Fe_3O_4 under magnetic field: effect of concentration and particle size of nano-Fe_3O_4. Cem Conc Comp 120:104036. https://doi.org/10.1016/j.cemconcomp.2021.104036
28. Jiao D, Lesage K, Yucel Yardimci M, El Cheikh K, Shi C, De Schutter G (2020) Rheological properties of cement paste with nano-Fe_3O_4 under magnetic field: flow curve and nanoparticle agglomeration. Materials 13(22): 5164. https://doi.org/10.3390/ma13225164
29. Laun HM, Gabriel C, Kieburg C (2010) Twin gap magnetorheometer using ferromagnetic steel plates: performance and validation. J Rheol 54(2):327–354. https://doi.org/10.1122/1.3302804
30. Mangal S, Kataria M (2018) Characterization of magnetorheological finishing fluid for continuous flow finishing process. J Appl Fluid Mech 11(6):1751–1763. https://doi.org/10.29252/jafm.11.06.28928
31. Rankin PJ, Horvath AT, Klingenberg DJ (1999) Magnetorheology in viscoplastic media. Rheol Acta 38(5):471–477. https://doi.org/10.1007/s003970050198
32. Roussel N, Lemaître A, Flatt RJ, Coussot P (2010) Steady state flow of cement suspensions: a micromechanical state of the art. Cem Conc Res 40(1):77–84. https://doi.org/10.1016/j.cemconres.2009.08.026
33. Jiao D, Shi C, Yuan Q (2019) Time-dependent rheological behavior of cementitious paste under continuous shear mixing. Const Build Mater 226:591–600. https://doi.org/10.1016/j.conbuildmat.2019.07.316
34. Coussot P, Ancey C (1999) Rheophysical classification of concentrated suspensions and granular pastes. Phys Rev E 59(4):4445–4457
35. Perrot A, Lecompte T, Khelifi H, Brumaud C, Hot J, Roussel N (2012) Yield stress and bleeding of fresh cement pastes. Cem Conc Res 42(7):937–944. https://doi.org/10.1016/j.cemconres.2012.03.015
36. McDermott WT, Butterbaugh JW (2008) Cleaning using argon/nitrogen cryogenic aerosols Developments in surface contamination and cleaning. William Andrew Publishing, Norwich, pp 951–986
37. Leite FL, Bueno CC, Da Roz AL, Ziemath EC, Oliveira ON (2012) Theoretical models for surface forces and adhesion and their measurement using atomic force microscopy. Int J Mol Sci 13(10):12773–12856. https://doi.org/10.3390/ijms131012773
38. Van Der Vurst F (2017) The mechanisms governing the robustness of fresh self-compacting concrete. Ghent University, Ghent
39. Bombard AJF, Knobel M, Alcantara MR, Joekes I (2002) Evaluation of magnetorheological suspensions based on carbonyl iron powders. J Intell Mater Syst Struct 13(7–8):471–478. https://doi.org/10.1106/104538902030706
40. Ashtiani M, Hashemabadi SH, Ghaffari A (2015) A review on the magnetorheological fluid preparation and stabilization. J Magn Magn Mater 374:716–730. https://doi.org/10.1016/j.jmmm.2014.09.020